Crimson Publishers
Wings to the Research

Research Article

Low-Temperature Preparation of β-C_2S from Sand/Lime Mixture: Influence of Sodium Hydroxide

Tantawy MA*

Chemistry Department, Egypt

ISSN : 2688-8394

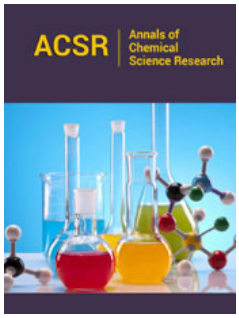

***Corresponding author:** Tantawy MA, Chemistry Department, Egypt

Submission: May 11 2019

Published: May 28, 2019

Volume 1 - Issue 3

How to cite this article: Tantawy MA. Low-Temperature Preparation of β-C_2S from Sand/Lime Mixture: Influence of Sodium Hydroxide. Ann Chem Sci Res. 1(2).ACSR.000512.2019.
DOI: 10.31031/ACSR.2019.01.000512

Abstract

The low-temperature preparation of belite (β-C2S) from a mixture of lime and white sand (Ca/Si=2) in presence of 0.5-5 M NaOH solution was investigated by hydrothermal treatment in a stainless steel capsule at 135 ˚C for 3 hours followed by calcination at 1000 ˚C for 3 hours. All materials were analyzed by FTIR, SEM-EDX, and XRD with semi-quantitative phase analysis calculation. The addition of NaOH changed the composition of the hydrothermal and calcination products. Different percent of β-C2S and other calcium and sodium silicate phases were produced with increasing the concentration of NaOH. In presence of 0.5M NaOH, 32.6% of β-C2S formed with the formation of calcium silicate with mole ratio CaO/SiO2=1.5 (rankinite, 30.9%) and sodium-calcium silicate (combeite, 8.6%). Whereas, in the presence of 5M NaOH, the hydrothermal reaction between lime and silica was effectively deactivated i.e. 32.9% of β-C2S formed. The formation of sodium silicate (31%), rankinite (15.4%) and sodium-calcium silicate (16.7%) phases were encouraged. The optimum condition for preparation of low-temperature β-C2S rich cement from lime and sand under these conditions can be achieved by the addition of 2M NaOH were, 77.7% of β-C2S formed and 12.4% combeite.

Keywords: White sand; Lime; Hydrothermal treatment; Calcination

The Common Phases that Appeared in the study and their Formula

Phase	Formula
Afwillite	$Ca_3Si_2O_8(OH)_2(H_2O)_2$
Alite, C_3S	Ca_3SiO_5
Belite (β-C_2S)	Ca_2SiO_4
Calcite	$CaCO_3$
Combeite	$Na_4Ca_4(Si_6O_{18})$
Dellaite	$Ca_6(SiO_4)\ (Si_2O_7)\ (SiO_4)\ (OH)_2$
α-Dicalcium silicate hydrate	$Ca_2(HSiO_4)\ (OH)$
Gehlenite	$Ca_2Al\ [AlSiO_7]$
Hillebrandite (dicalcium silicate hydrate)	$Ca_2(SiO_3)\ (OH)_2$
Kaolinite	$Al_2Si_2O_5(OH)_4$
Lime	CaO
Mayenite	$Ca_{12}Al_{14}O_{33}$
Portlandite	$Ca\ (OH)_2$
Quartz	SiO_2
Rankinite	$Ca_3Si_2O_7$
Sodium-calcium silicate	$Na_2Ca_3(Si_3O_{10})$
Sodium-hydrogen silicate hydrate	$Na_2(H_2SiO_4).7H_2O$
Xonotlite	$Ca_6Si_6O_{17}(OH)_2$

Introduction

Cement industry consumes large amounts of limestone and clay raw materials. About 1.5ton of limestone and 0.3ton of clay are needed for the production of 1ton of cement [1]. In addition, the cement industry consumes large amounts of energy (3100-3600 kJ/kg clinker) and produces significant quantities of CO_2 from the combustion of fuel and decomposition of limestone in cement manufacture (0.83 ton of CO_2/ton of cement). CO_2 contributes to global warming by increasing the greenhouse effect [2]. The world cement industry contributes about 8% of the global quantity of CO_2 emitted into the atmosphere [3]. Both the reduction of energy consumption as well as CO_2 emission in the cement production can be achieved by reducing the lime saturation factor (LSF) of the raw meal, which leads to the production of belite-rich clinker because the formation of belite occurs at a lower temperature than that for alite [4,5]. Alite is the most important component of Portland cement, though its formation needs high temperature and consumes comparatively large amounts of energy compared to belite. The enthalpy of formation of alite and belite is -1810kJ/kg and -1350kJ/kg respectively [6]. The decrease of the clinkering temperature belite cement during the production of belite cement results in energy savings up to 16% [7] and reduction of CO_2 emissions (up to 6-10%) [8]. This is the reason of great efforts towards the development of belite cement. Nevertheless, a slow hydration process and low strength after 28 days are disadvantages of the belite-rich cement. However, this kind of cement is suitable for long term sustainable materials [9].

C_2S exists in several polymorphic forms (α, $α›_L$, $α›_H$, β, and γ), that are stable in different temperature ranges with different hydraulic properties Figure 1. The γ-form is considered as inert and has poor hydraulic properties [10]. The $α›_L$, $α›_H$, and β-C_2S have a reactivity similar to that of alite [11]. The reactive forms of dicalcium silicate can be stabilized by rapid cooling of the belite clinker, at least 500 ˚C/min in the temperature range 1300-700˚C [12], or by inclusion of an appropriate stabilizer oxides into the crystal lattice of C_2S, which stabilize α′ and β polymorphs of C_2S such as B_2O_3, Na_2O, K_2O, P_2O_3, MgO, and BaO [10,13]. β-phase of belite cement is considered as one of the favorable constituents in industrial Portland cement clinker because it has a slow rate of hydration at early ages). Accordingly, it has a lower rate of heat evolution during cement hydration and it has improved mechanical strength [14]. Belite cement is also used in the production of refractory materials [15], heat resistant coatings [16], bioactive self-setting materials [17] and electrical insulators [18].

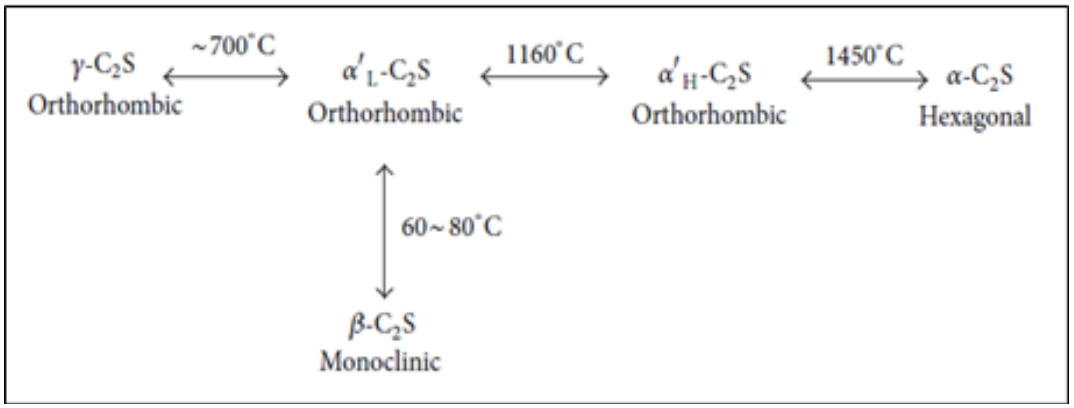

Figure 1: Thermal transformation relationship of belite Polymorphs.

Traditionally, belite is readily prepared from limestone and sand by solid-state reaction at high temperature by using different chemical stabilizing agents [19]. Whatever, this method leads to the formation of non-homogeneous products with impurity [20]. Alternatively, belite is readily prepared from CaO and SiO_2 by various routes at relatively lower temperatures such as hydrothermal-calcination process at 700-1000 °C [21-25], sol-gel synthesis [26], Pechini process [27] and hydrothermal-mechanochemical process [28-31]. However, the application of such methods on an industrial scale is complicated due to the high purity requirements of the starting material and complex equipment [32].

The reactive low energy belite cement represents great economic and environmental value due to the use of wastes and by-products such as fly ash [33,34]. It should be emphasized that the synthesis of belite by a hydrothermal-calcination method is one of the energetically cost-effective routes, because the temperature of hydrothermal synthesis does not exceed 200 °C and the temperature of the thermal activation is lower than 1000 °C [32]. One of the older trials for preparation of β-C_2S by hydrothermal-calcination route was done by Nanru [35] when they prepared β-C_2S by heating the hydrothermally produced dicalcium silicate hydrate (hillebrandite) at 950 °C with the molar ratio C/S=2. The obtained β-C_2S had a high specific surface and reacted with water as quickly as tricalcium silicate but starting from the 14th day of hydration [35]. Then Ishida as well as and Sasaki [36-38] obtained β-C_2S by heating hillebrandite at 600 °C. Those researchers showed that the intermediate phases after the hydrothermal process are very crucial to obtain various types and characteristics of products after calcinations. From these previous works, the α-dicalcium silicate hydrate, hillebrandite and dellaite phases as intermediate phases were obtained by hydrothermal treatment at temperatures between 100-250 ºC. Hillebrandite phase is recommended to produce more reactive C_2S than α-dicalcium silicate hydrate and dellaite phases. Kurdowski [39] heated the mixture of C-S-H phase with C/S molar ratio about 1.6 and CH at 800 ˚C, producing practically pure β-C_2S having a very high specific surface.

Sodium and potassium ions form solid solutions with dicalcium silicate, which imparts higher hydraulic activity and, especially in case of sodium, give much higher heat of hydration [39]. Other researchers have studied the synthesis of reactive belite by a hydrothermal-calcination method using coal combustion fly ash [40-50]. During the hydrothermal treatment, the pozzolanic reaction of fly-ash with lime is strongly activated, thus leading to the formation of hydraulic precursors. The dehydration of the hydraulic precursors at higher temperature 700-1000 ˚C, leads to the formation of reactive belite ($\alpha\rangle_L$ and β-Ca_2SiO_4) and mayenite. The compressive strength of this cement at 28 days reaches similar values to those for Portland cement CEM I 32.5 type [42] and has good resistance to sulfate attack [46]. Cement with $\alpha\rangle_L$-C_2S was prepared from fly ash in KOH solution (0.6M) at 5h at 100 ˚C, followed by burning at a minimum temperature of 800 ˚C and air-cooling produced reactive belite cement containing between 79% and 86% of C_2S ($\alpha\rangle_L$ and/or β polymorphs), the rest being $C_{12}A_7$ (5-8%), C_4AF (7-11%) and free lime (2%) [48,50]. Filkova [49] proved that the bottom ash with high CaO content fixed in anhydrite form (44.1%) is not suitable as raw material for synthesizing belite cement. Because the formation of gehlenite phase was observed at 900 °C, that is known as a retarder of cement hydration, and therefore undesirable for the cement [49]. Highly reactive β-belite is obtained with relatively high surface area (4.073 m^2g^{-1}) from lime sludge (a pulp and paper industry residue) and silica fume in a molar ratio of calcined at 2.0 by hydrothermal method followed by calcination at 1000 °C for 2h [21]. Also, β-C_2S was prepared from different siliceous raw materials such as silica fume, white sand, rice husk ash, silica, and amorphous silica under various hydrothermal conditions with lime in presence in stabilizer such as $BaCl_2$ followed by calcination of the product at 650 ˚C-1000 ˚C [24,51-55]. The aim of this work is to investigate the influence of NaOH concentration on the preparation of belite cement from lime and white sand hydrothermally treated and calcined at low temperatures.

Materials and Experimental Techniques

The raw materials that are used in this study are high-grade lime and white sand. The lime was produced by calcination of limestone powder in a muffle furnace at 950 ˚C, cooled to room temperature in a desiccator, milled to a fine powder and stored in a tightly closed plastic bag to avoid carbonation. The white sand was also milled to a fine powder. Figure 2 illustrates the procedure of the low-temperature synthesis of belite. A mixture of lime and white sand with a mole ratio (Ca/Si=2) and distilled water was added to obtain the water/solid ratio of 5/1 by weight. NaOH pellets were added to obtain 0.5, 2 and 5M concentration. The mixture was placed in a stainless-steel capsule keeping the occupied volume equals 67% of total volume capacity. The capsule was tightly closed, shacked vigorously, and hydrothermally treated at 135 ˚C for 3 hours in an electric oven. The capsule was removed from the oven and cooled to room temperature.

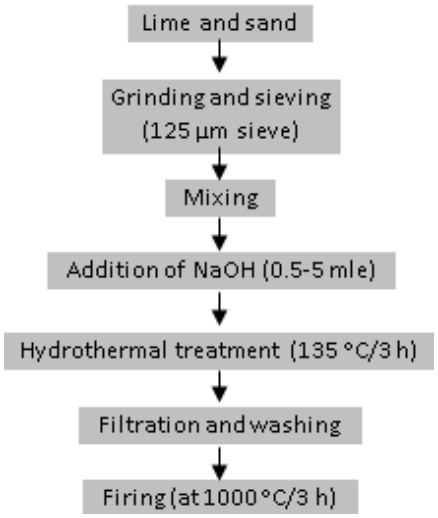

Figure 2: Procedure of low temperature synthesis of belite.

The hydrated product was filtered, washed with distilled water and dried in an electric oven overnight at 80 ˚C. The hydrated product was calcined in the muffle furnace at 1000 ˚C for 3 hours and cooled to room temperature in a desiccator, milled and stored in tightly closed plastic bags. The raw materials were analyzed by XRF techniques whereas the raw materials and calcined product were analyzed by FTIR, XRD, TGA/Dr TGA/DSC, and SEM-EDX techniques. X-ray fluorescence analysis (XRF) was measured by Philips PW1606 x-ray fluorescence spectrometer. X-ray diffraction analysis (XRD) was measured by Philips x-ray diffractometer PW 1370, Co. with Ni-filtered CuK_α radiation (1.5406 Å). Semi-quantitative phase analysis was calculated using the Bruker AXS configuration program. Fourier transform infrared analysis (FTIR) was measured by spectrometer Perkin Elmer FTIR System Spectrum X in the range 400-4000cm^{-1}. Thermogravimetric analysis/differential scanning calorimetry analysis (TGA/DrTGA/DSC) were measured by Netzsch STA 409 C/CD analyzer with 2 ˚C/min heating rate from room temperature up to 1000 ˚C, under air atmosphere at 50ml/min flow rate, the hold time at the appropriate temperature is zero. Scanning electron microscope with energy dispersive X-ray analysis (SEM-EDX) was measured by Jeol-Dsm 5400 LG apparatus.

Results

Table 1 illustrates the chemical composition of lime and white sand determined by XRF analysis. The lime composes of 86.64% CaO and the white sand composes of 98.27% SiO_2. Figure 3 illustrates the FTIR spectra of raw materials as well as the hydrothermally treated and calcined products. In the case of lime, the absorption band at 3644cm^{-1} is attributed to the vibration of OH-associated with hydrated lime present as partial hydration of lime [53]. The absorption bands at 876 and 1468cm^{-1} are attributed to the v^2 and v^3 vibration of carbonate (CO_3^{2-}) present as a result of the partial carbonation of lime [56]. The absorption band at 458cm^{-1} is attributed to the Ca-O stretching vibration [57]. The absorption bands at 1630 and 3425cm^{-1} are attributed to the stretching and bending vibrations of structural hydroxyl groups and water [58]. The absorption band at 1420cm^{-1} is attributed to the Ca-OH vibration band of lime [59]. In case of sand, the absorption bands at 1087, 787, 472cm^{-1} are attributed to the Si-O-Si asymmetric stretching vibration, Si-O-Si symmetric stretching vibration and O-Si-O bending vibration of quartz [60]. The absorption bands at 689, 540cm^{-1} are attributed to the Si-O vibration of kaolinite. The absorption band at 1032cm^{-1} is attributed to the Si-O stretching (in-plane) vibration of kaolinite.

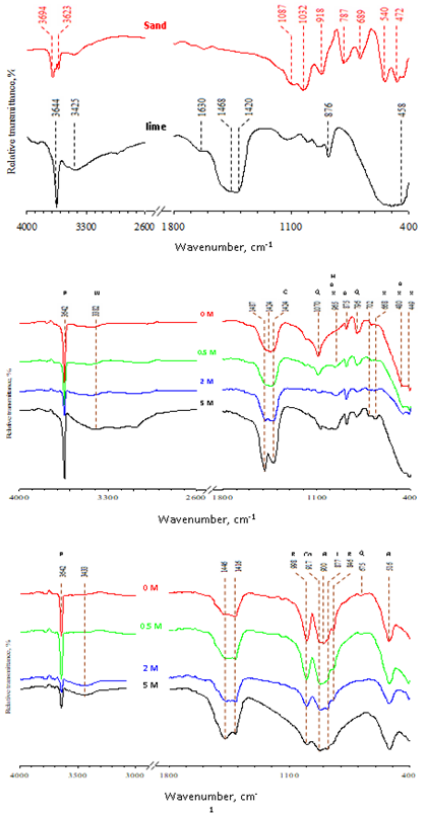

Figure 3: FTIR spectra of (a) lime and sand, (b) hydrothermally treated and (c) calcined products.
(A afwillite, ββ-C2S, C calcite, Co combeite, H calcium silicate hydrate, L lime, P portlandite, Q quartz, R rankinite, W water and X xonotlite).

Table 1: Chemical composition of lime and sand determined by XRF.

Oxide, Wt %	SiO2	Al2O3	CaO	Fe2O3	MgO	SO3	Na2O	K2O	TiO2	Cl-	LOI*	Total
Lime	1.90	0.67	90.64	0.32	0.71	0.44	0.24	0.08	0.04	0.08	4.24	99.58
Sand	98.20	0.95	0.31	0.08	0.11	0.07	0.10	0.01	0.02	-	0.05	99.88

*LOI is the loss on ignition.

The absorption band at 918cm^{-1} is attributed to the AlAlOH vibration of kaolinite [61]. The absorption bands at 3694, 3623cm^{-1} are attributed to the stretching vibrations of surface OH groups and stretching vibrations of inner hydroxyl groups [62]. In the case of the hydrothermally treated products, the absorption band at 965cm^{-1} is attributed to the characteristic vibration of calcium silicate hydrate. The absorption bands at 796, 1070cm^{-1} are attributed to the residual quartz. The absorption band at 3642cm^{-1} is attributed to residual portlandite. The absorption band at 1424cm^{-1} is attributed to calcite formed due to partial carbonation of portlandite. The absorption band at 3382cm^{-1} is attributed to the vibration band of water molecules. The absorption bands at 480, 875, 965cm^{-1} are attributed to the characteristic vibration bands of afwillite. The absorption bands at 449, 480, 668, 965cm^{-1} are

attributed to the characteristic vibration bands of xonotlite. In the case of the calcined products, the absorption bands at 1006, 876, 520cm^{-1} are attributed to the characteristic vibration bands of β-C_2S [63].

The absorption band at 917cm^{-1} is attributed to the characteristic vibration band of combeite. The absorption bands at 846, 998cm^{-1} are attributed to the characteristic vibration bands of rankinite. The absorption bands at 796, 1070cm^{-1} are attributed to the residual quartz and the absorption band at 877cm^{-1} is attributed to the residual lime. Figure 4 illustrates the XRD diffraction patterns of raw materials as well as the hydrothermally treated and calcined products. Lime composes mainly of CaO and sand composes of quartz. The main crystalline phases that were detected in the hydrothermally treated products are the afwillite and xonotlite minerals in addition to residual portlandite and quartz. The main crystalline phases that were detected in the calcined products are the rankinite, β-C_2S, combeite, sodium-hydrogen silicate hydrate, sodium-calcium silicate minerals in addition to residual calcite, portlandite, lime, and quartz. Table 2 illustrates the semi-quantitative phase analysis derived from XRD results. The addition of NaOH markedly affects the rate of hydrothermal reaction between lime and silica as well as the formation of β-C_2S and other phases such as rankinite (calcium silicate with mole ratio CaO/SiO_2=1.5), combeite, sodium-calcium silicate, and sodium silicate.

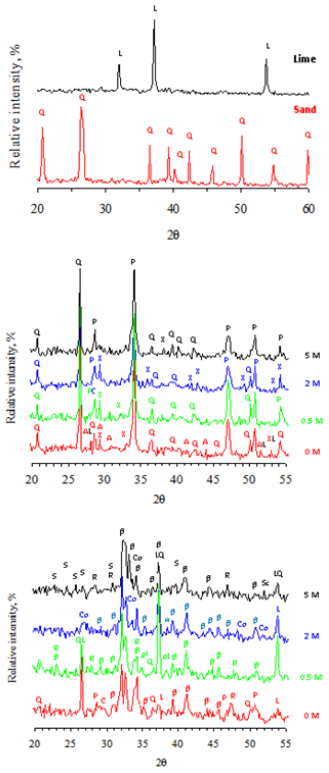

Figure 4: XRD diffraction patterns of (a) lime and sand, (b) hydrothermally treated and (c) calcined products.
(An afwillite, β β-C2S, C calcite, Co combeite, L lime, P portlandite, Q quartz, R rankinite, S sodium-hydrogen silicate hydrate, Sc sodium-calcium silicate and X xonotlite).

Table 2: The semi quantitative phase analysis.

Phases	NaOH Conc.			
	0M	0.5M	2M	5M
β-C2S	65	33	77	33
Quartz	16	9	-	-
Lime	4	14	10	4
Portlandite	10	4	-	-
CaCO3	5	-	-	-
Rankinite	-	31	-	15
Combeite	-	9	13	-
Sodium-calcium silicate	-	-	-	17
Sodium-hydrogen silicate hydrates	-	-	-	31

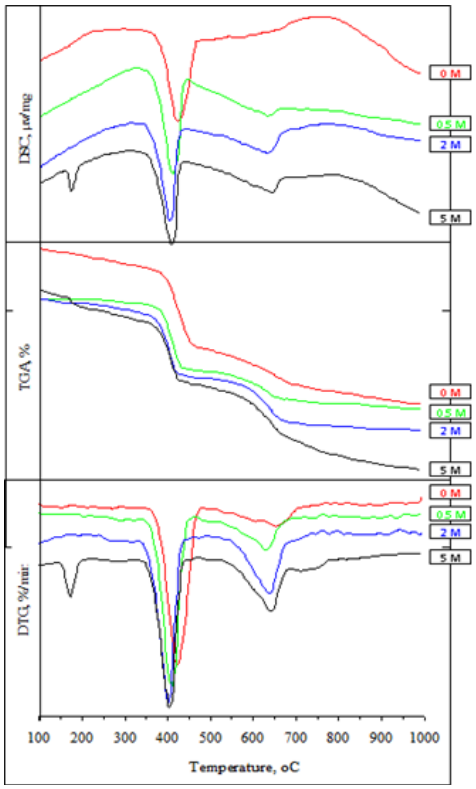

Figure 5: DSC, TGA and DTG of 0M-5M hydrothermally treated.

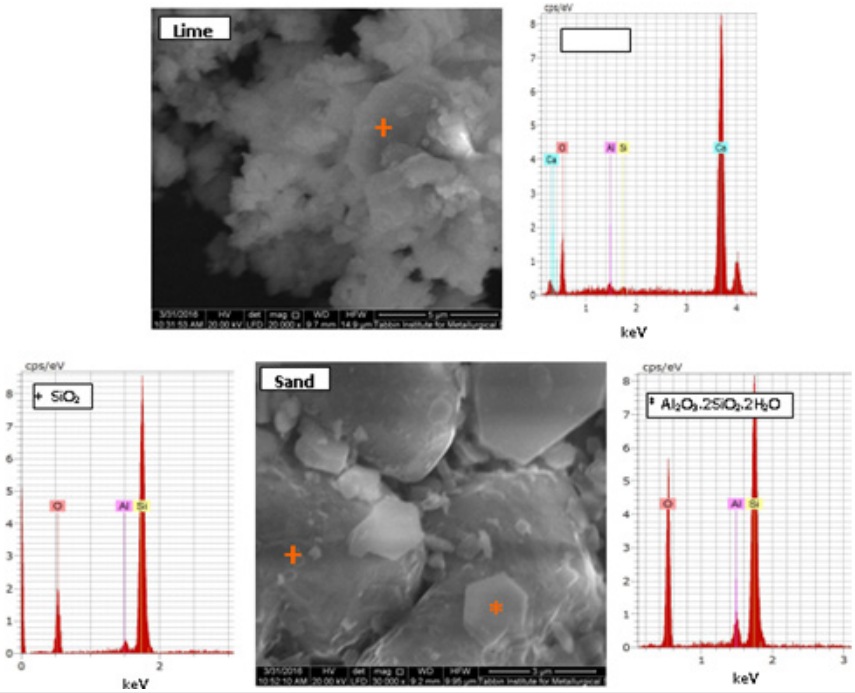

Figure 6a: SEM-EDX of lime and sand.

Figure 5 illustrates DSC/TGA/DrTGA thermograms of the hydrothermally treated product. The thermograms illustrate the two thermal reactions that occur during the calcination of all the hydrothermally treated products at about 408 ˚C and 643 ˚C. A clear endothermic peak occurs at about 173 ˚C in case of sand/lime mixture that was hydrothermally treated in presence of 5M NaOH. Figure 6a illustrates the SEM-EDX analysis of raw materials as well as the hydrothermally treated and calcined products. SEM results of lime show the morphology of lime grains. SEM results of white sand show the existence of hexagonal platelets of kaolinite crystals [64] laying on the surface of quartz aggregates. The SEM results of hydrothermally treated products show the existence of calcium silicate hydrate (hillebrandite) gel. SEM results of calcined products show the existence of fine β-C_2S aggregates.

Discussion

FTIR results of raw materials (Figure 6b) illustrate that lime is partially carbonated as proved from the appearance of the absorption bands at 876 and 1468cm^{-1} corresponding to the v^2 and v^3 vibration of carbonate. White sand contains residual kaolinite, which is found as an accessory mineral in white sand. During the hydrothermal treatment of white sand/lime mixture with the mole ratio of CaO/SiO_2=2 at 135 ˚C for 3 hours, the reaction between lime and silica was activated leading to the formation of calcium silicate hydrate, with the existence of residues of the starting materials (quartz and lime). The later under these conditions was hydrated (portlandite) as well as partially carbonated (calcite). The formation of other crystalline calcium silicate hydrates, i.e. afwillite and xonotlite also was encouraged under the hydrothermal conditions. The hydrothermal treatment of white sand/lime mixture in the presence of increasing concentrations of NaOH favors the formation of more calcium silicate hydrate at the expense of afwillite and xonotlite phases. The XRD results provided with the semi-quantitative phase analysis of the calcined products using the Bruker AXS configuration program give a relatively clear idea about the reactions and phase transformations which occur as a result of the hydrothermal treatment of lime/sand mixture (mole ration CaO/SiO_2=2) in presence of NaOH solution (0.5-5M) at 135 ˚C and calcination of the products at 1000 ˚C.

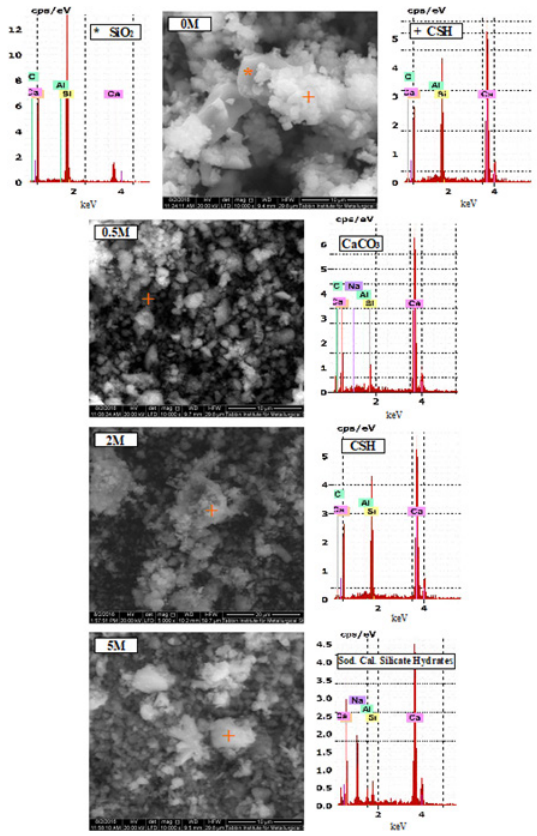

Figure 6b: SEM-EDX of 0M-5M hydrothermally treated.

In the absence of NaOH, 64.73% β-C_2S formed in the calcined product leaving behind appreciable percent of silica and lime that was partially hydrated (portlandite) and carbonated ($CaCO_3$) Figure 6c. This means that the reaction between quartz and lime does not reach the state of completion in the absence of NaOH. In the presence of 0.5M NaOH, the hydrothermal reaction between lime and silica was deactivated (32.6% β-C_2S was formed). On the other hand, the formation of calcium silicate with mole ratio CaO/SiO_2=1.5 (rankinite, 30.9%) as well as sodium-calcium silicate (combeite, 8.6%) was activated. In the presence of 2M NaOH, the hydrothermal reaction between lime and silica was markedly activated leading to the formation of the highest percentage of β-C_2S (77.7%) and 12.4% combeite. In the presence of 5M NaOH, the hydrothermal reaction between lime and silica was effectively deactivated leading to the formation of the lowest percent of β-C_2S (32.9%). In contrast, the formation of sodium silicate (31%), rankinite (15.4%), and sodium-calcium silicate (16.7%) phases were encouraged. Regarding the DSC/TGA/DrTGA thermograms of the hydrothermally treated products, the first endothermic peak is attributed to the dehydration of Portlandite [65]. The second endothermic peak is attributed to the formation of β-C_2S as a result of the dehydration of calcium silicate hydrate [66]. The endothermic peak that occurs at about 173 ˚C in case of sand/lime mixture that was hydrothermally treated in presence of 5M NaOH, is attributed to the loss of water bound in different ways to the sodium silicate in the range of 50-200 ˚C [67]. The raw materials, as well as the hydrothermally treated and calcined products, were analyzed by SEM-EDX. The empirical formulae of different phases that were pointed out were calculated using the EDX data expressed in normalized atom%.

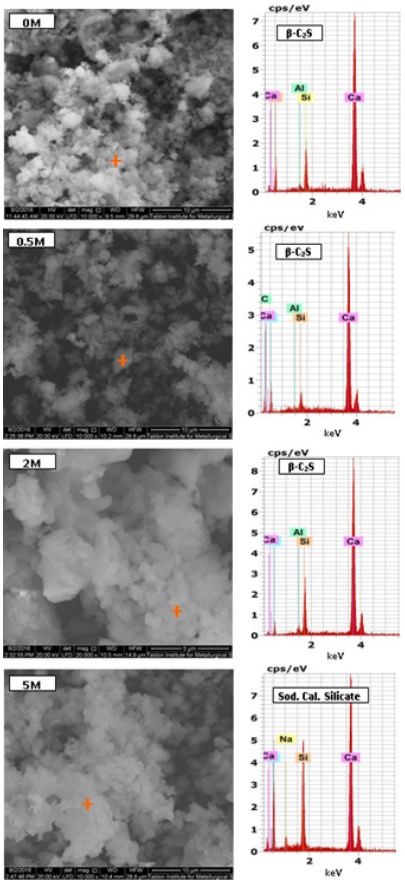

Figure 6c: SEM-EDX of 0M-5M hydrothermally ttreated and calcined at 850 ˚C.

Taking into consideration that the calculated formulae are approximate due to the presence of variable contents of foreign ions depending on the proximity of the EDX point analysis to the underlying other phases [68]. SEM results of raw materials show the morphology of fine lime grains as well as that of large quartz grains with the existence of hexagonal platelets of kaolinite crystals [64] laying on its surface. The SEM images of the hydrothermally treated white sand/lime mixture in the absence of NaOH reveal an abrupt change in the microstructure of the starting materials. This proves that the reaction between lime and silica was activated dissolving much of quartz grains and the formation of calcium silicate hydrate gel with the existence of unreacted quartz grains. SEM results show that the amount of calcium silicate hydrate gel reaches the maximum percentage at 2M NaOH addition. Increasing the concentration of NaOH to 5M leads to the formation of sodium-calcium silicate hydrates. SEM results of calcined products show the presence of β-C_2S. Also, the formation of β-C_2S reaches its maximum at 2M NaOH addition. Increasing the concentration of NaOH to 5M leads to the formation of sodium-calcium silicates instead of β-C_2S.

Conclusion

This paper study the low-temperature synthesis of belite by the hydrothermal treatment of lime/sand mixture (mole ration CaO/SiO_2=2) in presence of (0.5-5M) NaOH solution at 135˚C for 3 hours and calcination of the products at 1000 ˚C for 3 hours. The main conclusions of this investigation are:

A. The FTIR, TGA, SEM, and XRD results provided with the semi-quantitative phase analysis illustrate the different reactions and phase transformations that occur during the hydrothermal-calcination processes for the lime/sand mixture in presence of NaOH solution.

B. Without the addition of NaOH, the hydrothermal reaction between quartz and lime does not reach the state of completion. Hence, 64.73% β-C_2S formed in the calcined product leaving behind appreciable percent of unreacted silica and lime.

C. The addition of NaOH changed the composition of the hydrothermal and calcination products. Accordingly, different percent of β-C_2S and other calcium and sodium silicate phases were produced with raising the concentration of NaOH.

D. In presence of 0.5M NaOH, 32.6% β-C_2S was formed with the formation of calcium silicate with mole ratio CaO/SiO_2 =1.5 (rankinite, 30.9%) and sodium-calcium silicate (combeite, 8.6%).

E. In the presence of 2M NaOH, the higher percent of β-C_2S formed (77.7%) and 12.4% combeite.

F. In presence of 5M NaOH, the hydrothermal reaction between lime and silica was effectively deactivated leading to the formation of the lowest percent of β-C_2S (32.9%). Whereas, the formation of sodium silicate (31%), rankinite (15.4%), and sodium-calcium silicate (16.7%) phases were encouraged.

G. Accordingly, the optimum condition for preparation of low-temperature β-C_2S rich cement from lime and sand under these conditions can be achieved by the addition of 2M NaOH.

Further studies in the future must be conducted to investigate the reactivity and cementitious properties of belite prepared under the experimental procedure illustrated in this study.

References

1. British Geological Survey (2005) Mineral profile: cement raw materials. Keyworth: Office of the Deputy Prime Minister, p. 20.
2. Popescu CD, Muntean M, Sharp JH (2003) Industrial trial production of low energy belite cement. Cem Concr Compos 25(7): 689-693.
3. Heede R (2014) Tracing anthropogenic carbon dioxide and methane emissions to fossil fuel and cement producers. Climatic Change 122: 229-241.
4. Kacimi L, Simon-Masseron A, Salem S, Ghomari A, Derriche Z (2009) Synthesis of belite cement clinker of high hydraulic reactivity. Cem Concr Res 39(7): 559-565.
5. Staněk T, Sulovský P (2015) Active low-energy belite cement. Cem Concr Res 68: 203-210.
6. Barin I, Knage O, Kubaschewski O (1977) Thermochemical properties of inorganic substances. New York, USA.
7. Uchikawa H (1994) Management strategy in cement technology for the next century: part 3. World Cem, 47.
8. Gartner E (2004) Industrially interesting approaches to "low-CO_2" cements. Cem Concr Res 34(9): 1489-1498.
9. Neville AM (1985) Properties of Concrete (3rd edn), Prentice Hall, New York, USA.
10. Odler I (1998) Hydration, setting and hardening of Portland cement. In: Hewlett PC (Ed.), Lea's Chemistry of Cement and Concrete, (4th edn), Arnold, London, UK, pp. 241-297.
11. Chatterjee AK (1996) High belite cements-present status and future technological options: Part I. Cem Concr Res 26(8): 1213-1225.
12. Lawrence CD (2003) The Production of Low-energy Cements. Lea's Chemistry of Cement and Concrete. (4th edn), Butterworth-Heinemann, Oxford, USA.
13. Cuesta A, Losilla ER, Aranda MAG, Sanz J, De la Torre AG (2012) Reactive belite stabilization mechanisms by boron-bearing dopants. Cem Concr Res 42(4): 598-606.
14. Guerrero A, Goni S, Dolado JS (2009) Belite Cements: Modifications of calcium silicate hydrate (CSH) gel by alkaline hydrothermal activation. ACI Mater J 106(2): 138.
15. Rodrıguez JL, Rodrıguez MA, De Aza S, Pena P (2001) Reaction sintering of zircon-dolomite mixtures. J Eur Ceram Soc 21(3): 343-354.
16. Vogan JW, Hsu L, Stetson AR (1981) Thermal barrier coatings for thermal insulation and corrosion resistance in industrial gas turbine engines. Thin Solid Films 84: 75-87.
17. Gou Z, Chang J, Zhai W, Wang J (2005) Study on the self-setting property and the in vitro bioactivity of β-Ca_2SiO_4. J Biomed Mater Res B 73: 244-251.
18. Negmatov NS, Abdullaev ZZ (2001) High-voltage electric insulators based on wollastonite. Glass Ceram 58: 396-397.
19. Maheswaran S, Kalaiselvam S, Arunbalaji S, Palani GS, Iyer NR (2015) Low temperature preparation of belite from lime sludge and Nano silica through solid-state reaction. J Therm Anal Calorim 119: 1845-1852.
20. Liu X, Tao S, Ding C (2002) Bioactivity of plasma sprayed dicalcium silicate coatings. Biomaterials 23: 963-968.
21. Maheswaran S, Kalaiselvam S, Saravana Karthikeyan SKS, Kokila C, Palani GS (2016) β-belite cements (β-dicalcium silicate) obtained from calcined lime sludge and silica fume. Cement and Concrete Composites 66: 57-65.
22. Rodrigues FA (2003) Low-temperature synthesis of cements from rice hull ash. Cem Concr Res 33(10): 1525-1529.
23. Guerrero A, Goñi S, Campillo I, Moragues A (2004) Belite cement clinker from coal fly ash of high Ca content. Optimization of synthesis parameters. Environ Sci Tech 38(11): 3209-3213.
24. Singh NB (2006) Hydrothermal synthesis of β-dicalcium silicate (β-Ca_2SiO_4). Prog Crystal Growth Ch 52: 77-83.
25. Pimraksa K, Hanjitsuwan S, Chindaprasirt P (2009) Synthesis of belite cement from lignite fly ash. Ceram Int 35(6): 2415-2425.
26. Chrysafi R, Perraki T, Kakali G (2007) Sol-gel preparation of 2CaO·SiO_2. J Eur Ceram Soc 27: 1707-1710.
27. Nettleship I, Shull JL, Kriven WM (1993) Chemical preparation and phase stability of Ca_2SiO_4 and Sr_2SiO_4 powders. J Eur Ceram Soc 11: 291-298.
28. Guerrero A, Goni S, Moragues A, Dolado JS (2005) Microstructure and mechanical performance of belite cements from high calcium coal fly ash. J Am Ceram Soc 88: 1845-1853.
29. Sritharan T, Boey FYC, Srinivas A (2007) Synthesis of complex ceramics by mechanochemical activation. J Mater Process Tech 192: 255-258.
30. Stevulova N, Filkova I, Baltakys K (2012) Low-temperature synthesis of belite cement from reactive mixtures based on coal fly ash. J Civil Eng Arch 6: 190-196.
31. El-Didamony H, Khalil KA, Ahmed IA, Heikal M (2012) Preparation of β-dicalcium silicate (β-C_2S) and calcium sulfoaluminate (C3A3CS) phases using non-traditional nano materials. Constr Build Mater 35: 77-83.
32. Gendvilas R (2015) Synthesis, properties of α-C_2SH and its application for the production of hydraulic binder material, PhD Thesis, Department of Silicate Technology, Faculty of Chemical Technology, Kaunas University of Technology, Lithuania.
33. Goňi ES, Guerrero BA, Moragues TA, Campillo SI (2004) Belite cement clinker from coal fly ash of high ca content. Optimization of synthesis parameters. Environ Sci Technol 38: 3209-3213.
34. Števulová N (2009) Mechanochemical formation of calcium silicates in multicomponent mixtures. Chemine Technologija 51(2): 10-17.
35. Yang N, Zhong Baiqian Tild WZ (1986) 8th ICCC Rio de Janeiro. Rio de Janeiro 3: 22.
36. Ishida H, Mabuchi K, Sasaki K, Mitsuda T (1992) Low-temperature synthesis of β-Ca_2SiO_4 from Hillebrandite. J Am Ceram Soc 75: 2427-2432.
37. Ishida H, Yamazaki S, Sasaki K, Okada Y, Mitsuda T (1993) α-Dicalcium silicate hydrate: Preparation, decomposed phase, and its hydration. J Am Ceram Soc 76: 1707-1712.
38. Sasaki K, Ishida H, Okada Y, Mitsuda T (1993) Highly reactive β-dicalcium silicate: V, influence of specific surface area on hydration. J Am Ceram Soc 76: 870-874.
39. Kurdowski W, Duszak S, Trybalska B (1997) Belite produced by means of low-temperature synthesis. Cement and Concrete Research 27(1): 51-62.
40. Goni S, Guerrero A, Macias A, Luxan MP (1998) Effect of the synthesis temperature on the hydration reaction of fly ash-belite cement. In: Cohen M, Mindess S, Skalny J (Eds.), Materials Science of Concrete: The Sidney Diamond Symposium, American Ceramic Society, pp. 93-108.
41. Arjunan P, Silsbee MR, Roy DM (1999) Sulfoaluminate-belite cement from low calcium fly ash and sulfur-rich and other industrial by-products. Cem Concr Res 29(8): 1305-1311.

42. Guerrero A, Goni S, Macias A, Luxan MP (1999) Mechanical properties, pore size distribution, and pore solution of fly ash-belite cement mortars. Cem Concr Res 29(11): 1753-1758.

43. Guerrero A, Goni S, Macias A, Luxan MP (1999) Hydraulic activity and microstructural characterization of new fly ash-belite cements synthesized at different temperatures. J Mater Res 14: 2680-2687.

44. Guerrero A, Goni S, Macias A, Luxan MP (2000) Effect of the starting fly ash on the microstructure and mechanical properties of fly ash-belite cement mortars. Cem Concr Res 30(4): 553-559.

45. Goni S, Guerrero A, Luxan MP, Macias A (200) Dehydration of pozzolanic products hydrothermally synthesized from fly ashes: microstructure evolution. Mater Res Bull 35: 1333-1344.

46. Guerrero A, Goni S, Macias A (2000) Durability of new fly ash–belite cement mortars in sulfated and chloride medium. Cem Concr Res 30(8): 1231-1238.

47. Byrappa K, Adschiri T (2007) Hydrothermal technology for nanotechnology. Prog Cryst Growth Charact Mater 53: 117-166.

48. Kacimi L, Cyr M, Clastres P (2010) Synthesis of α›L-C2S cement from fly-ash using the hydrothermal method at low temperature and atmospheric pressure. Journal of Hazardous Materials 181: 593-601.

49. Filkova I, Stevulova N (2011) Possibilities of coal fly ash utilization in the low temperature belite cement production. The 8th International Conference of Environmental Engineering, Vilnius, Lithuania, pp. 90-93.

50. Mazouzi W, Kacimi L, Cyr M, Clastres P (2014) Properties of low temperature belite cements made from aluminosilicate wastes by hydrothermal method. Cement and Concrete Composites 53: 170-177.

51. Tantawy MA, Shatat MR, El-Roudi AM, Taher MA, Abd-El-Hamed M (2012) Low Temperature synthesis of belite cement based on silica fume and lime. International Scholarly Research Notices.

52. Tantawy MA (2014) Low Temperature synthesis of belite cement from white sand and lime. Int J Eng Res Tech 3: 1351.

53. Tantawy MA (2015) Influence of silicate structure on the low temperature synthesis of belite cement from different siliceous raw materials. Journal of Materials Science and Chemical Engineering 3: 98-106.

54. Georgescu M, Tipan J, Badanoiu A, Crisan D, Dragan I (2000) Highly reactive dicalcium silicate synthesised by hydrothermal processing. Cement and Concrete Composites 22(5): 315-319.

55. Rodrigues FA, Monteiro PJM (1999) Hydrothermal Synthesis of Cements from Rice Hull Ash. Journal of Materials Science Letters 18(19): 1551-1552.

56. Gupta A, Singh P, Shivakumara C (2010) Synthesis of $BaSO_4$ nanoparticles by precipitation method using sodium hexametaphosphate as a stabilizer. Solid State Communications 150: 386-388.

57. Rodrigues FA (1999) Synthesis of cements from rice hull. Symposia papers presented before the division of environmental chemistry. American Chemical Society 39: 30-31.

58. Madejova J, Komadel P (2001) Baseline studies of the clay minerals society source clays: infrared methods. Clays and Clay Minerals 49(5): 410-432.

59. Gunasekaran S, Anbalagan G (2007) Spectroscopic characterization of natural calcite minerals. Spectrochimica Acta (Part A) 68(3): 656-664.

60. Baltakys K, Jauberthie R, Siauciunas R, Kaminskas R (2007) Influence of modification of SiO_2 on the formation of calcium silicate hydrate. J Mater Sci Pol 25: 663.

61. Eisazadeh A, Kassim KA, Nur H (2012) Solid-state NMR and FTIR studies of lime stabilized montmorillonitic and lateritic clays. Applied Clay Science 67-68: 5-10.

62. Frost RL, Kristof J, Paroz GN, Tran TH, Kloprogge JT (1998) The role of water in the intercalation of kaolinite with potassium acetate. Colloid Interface Sci 204(2): 227-236.

63. Fernandez L, Alonso C, Hidalgo A, Andrade C (2005) The role of magnesium during the hydration of C_3S and C-S-H formation. Scanning electron microscopy and mid-infrared studies. Advances in Cement Research 17: 9-21.

64. Thompson JG, Uwins PJR, Whittaker AK, Mackinnon IDR (1992) Structural characterization of kaolinite-NaCl intercalate and its derivatives. Clays and Clay Minerals 40(4): 369-380.

65. Heikal M, El-Didamony H, Morsy MS (2000) Limestone-filled pozzolanic cement. Cem Concr Res 30(11): 1827-1834.

66. Taylor HFW (1998) Cement Chemistry. In: (2nd edn), Thomas Telford Publishing, London, UK.

67. Aulisa Ê, Gilliam D (2015) A practical guide to geometric regulation for distributed parameter systems. Chapman and Hall/CRC.

68. Donatello S, Kuenzel C, Palomo A, Fern□ndez-Jiménez A (2014) High temperature resistance of a very high-volume fly ash cement paste. Cement and Concrete Composites 45: 234-242.